World Journal of Radiology

Online Submissions: http://www.wjgnet.com/esps/
wjr@wjgnet.com
doi:10.4329/wjr.v5.i3.68

World J Radiol 2013 March 28; 5(3): 68-80
ISSN 1949-8470 (online)

TOPIC HIGHLIGHT

Khaled M Elsayes, MD, *Series Editor*

Abdominal applications of diffusion-weighted magnetic resonance imaging: Where do we stand?

Ajaykumar C Morani, Khaled M Elsayes, Peter S Liu, William J Weadock, Janio Szklaruk, Jonathan Russell Dillman, Asra Khan, Thomas L Chenevert, Hero K Hussain

Ajaykumar C Morani, Khaled M Elsayes, Janio Szklaruk, Department of Radiology, University of Texas, MD Anderson Cancer Center, Houston, TX 77030, United States
Peter S Liu, William J Weadock, Jonathan Russell Dillman, Asra Khan, Thomas L Chenevert, Hero K Hussain, Department of Radiology, University of Michigan, Ann Arbor, MI 48109, United States
Author contributions: Morani AC designed, wrote and researched the paper as well as searched the literature; Elsayes KM designed, contributed to adrenal portion; Liu PS contributed to pancreas portion; Elsayes KM, Liu PS, Weadock WJ, Szklaruk J, Dillman JR, Chenevert TL and Hussain HK edited and checked the manuscript; Khan A contributed to kidney portion of the paper.
Correspondence to: Ajaykumar C Morani, MD, MBBS, DNB, Department of Radiology, University of Texas, MD Anderson Cancer Center, Houston, TX 77030, United States. ajaycmorani@yahoo.com
Telephone: +1-713-7452509 Fax: +1-713-7944379
Received: September 29, 2012 Revised: October 21, 2012
Accepted: January 31, 2013
Published online: March 28, 2013

Abstract

Diffusion-weighted imaging (DWI) is one of the magnetic resonance imaging (MRI) sequences providing qualitative as well as quantitative information at a cellular level. It has been widely used for various applications in the central nervous system. Over the past decade, various extracranial applications of DWI have been increasingly explored, as it may detect changes even before signal alterations or morphological abnormalities become apparent on other pulse sequences. Initial results from abdominal MRI applications are promising, particularly in oncological settings and for the detection of abscesses. The purpose of this article is to describe the clinically relevant basic concepts of DWI, techniques to perform abdominal DWI, its analysis and applications in abdominal visceral MR imaging, in addition to a brief overview of whole body DWI MRI.

Key words: Diffusion-weighted imaging; Imaging; Diffusion

Morani AC, Elsayes KM, Liu PS, Weadock WJ, Szklaruk J, Dillman JR, Khan A, Chenevert TL, Hussain HK. Abdominal applications of diffusion-weighted magnetic resonance imaging: Where do we stand? *World J Radiol* 2013; 5(3): 68-80 Available from: URL: http://www.wjgnet.com/1949-8470/full/v5/i3/68.htm DOI: http://dx.doi.org/10.4329/wjr.v5.i3.68

INTRODUCTION

Diffusion is the constant and uninhibited random Brownian motion of water molecules. Diffusion of water at the molecular level in biological tissues is modified and limited by interactions with cell membranes and macromolecules[1,2]. Magnetic resonance imaging (MRI) diffusion-weighted imaging (DWI) uses the differences in the motion (diffusion) of water molecules in extracellular and intracellular fluid and vascular fluids to produce image contrast, with no need for exogenous contrast materials. This imaging technique provides both qualitative and quantitative information at the cellular level with regards to tissue cellularity and cell membrane integrity and is hence considered a form of functional imaging[1,3,4]. DWI has been predominantly used in the brain in the evaluation of stroke and can help diagnose ischemic changes before signal alterations of other pulse sequences and morphological abnormalities become apparent. Over the past decade, there has been increasing interest in the use of DWI for the evaluation of extracranial conditions due to a variety of technical advances, such as development of high amplitude gradients, multichannel surface coils and parallel imaging[1].

Diffusion is inversely related to cellularity, cell membrane integrity and lipophilicity[1-3]. Restricted (or imped-

ed) diffusion is observed in tissues with high cellularity, *e.g.*, tumors, abscesses, fibrosis and cytotoxic edema. Relatively free or unimpeded diffusion is found in tissues with low cellularity or disrupted cell membranes, such as cysts and necrotic tissues[1-3,5,6]. Intravascular water molecules have a larger diffusion distance and contribute more to the DWI signal than water molecules in the extracellular and intracellular spaces. Hence, tumors with high vascularity have higher DWI signals[1,3].

TECHNIQUE

DWI is based on T2-weighted imaging. For most clinical uses, a symmetrical pair of diffusion-sensitizing (bipolar) gradients is applied around the 180° refocusing pulse of a standard T2-weighted sequence. The phase shift induced by the first diffusion gradient in static water molecules is subsequently rephased by the second diffusion gradient. Hence, in static tissue, there is no significant change in measured signal intensity. In contrast, moving water molecules are not rephased by the second gradient (due to motion), resulting in signal loss. Thus, motion and signal loss are proportional and motion of water molecules is detected as a reduction in measured signal intensity[1,3].

Free breathing and breath-hold imaging techniques have been used for abdominal DWI. The breath hold (*e.g.*, single-shot fast-spin EPI with parallel imaging) sequences are commonly used in clinical practice and result in fewer motion artifacts and better anatomic detailing[1,3]. Hence, this technique is useful for detecting small lesions. Disadvantages include poor signal-to-noise ratio (SNR), artifacts due to pulsatility and susceptibility, and only a limited number of *b* values can be obtained per breath hold. Non-breath hold DWI techniques provide improved SNR and contrast-to-noise ratios, allowing for higher spatial resolution and the possibility of multiplanar reformatting. Multiple *b* values can also be easily obtained but this technique is prone to partial volume averaging artifact and can be time consuming[1,3]. Respiratory motion compensation techniques can be used to reduce motion artifacts.

With all DWI techniques, TR should be maintained long enough to minimize T1 saturation effects. The sensitivity of DWI to water motion is determined by the *b* value (mm^2/s), which reflects the influence of the diffusion sensitizing gradients and can be altered by changing gradient amplitude, gradient duration and time interval between the paired gradients[1,3]. For a meaningful interpretation, DWI needs to be performed using at least two *b* values: $b = 0$ mm^2/s and $b = 100$ to 1000 mm^2/s[1,3]. DWI performed with $b = 0$ mm^2/s is a T2-weighted sequence. At lower *b* values (200 mm^2/s or less), the calculated apparent diffusion coefficient (ADC) is influenced by tissue perfusion and water diffusivity. Increasing the *b* value over 200 mm^2/s reduces the effect of perfusion.

QUALITATIVE ASSESSMENT OF DWI

DWI images can be qualitatively assessed by visual inspection. Water molecules with a large degree of motion (*e.g.*, in blood vessels) have less signal attenuation (remain hyperintense or bright) at small *b* values (*e.g.*, $b = 50$-100 mm^2/s) and greater signal attenuation (become hypointense or dark) at large *b* values. Water molecules with slow and restricted (or impeded) motion (*e.g.*, in certain tumors) have less signal attenuation (remain hyperintense or bright) at large *b* values (*e.g.*, $b = 500$-1000 mm^2/s). Overall, the higher the *b* value, the more sensitive the sequence is to diffusion effects. Higher *b* values (*e.g.*, $b = 1000$) are also optimum for background signal suppression[1,3].

The relative change in DWI signal intensity at different *b* values can be used to characterize tissues on the basis of differences in water diffusion. For example, the cystic or necrotic fraction of a heterogeneous tumor will show greater signal attenuation (low signal intensity) on high *b*-value imaging than solid portions (high signal intensity). Thus, subjective visual assessment of the relative tissue signal changes on DWI using multiple *b* values may be useful for tumor detection, tumor characterization and assessment of treatment response[1]. However, observed DWI signal intensity depends not only on water diffusion, but also on T2 relaxation time (so-called "T2 shine-through" effect). "T2 shine-through" effect can result in high signal intensity on high *b* value DWI images without impeded diffusion. This may result in image interpretation errors, particularly if the ADC maps are not examined. ADC maps, which are actually a quantitative measure of tissue diffusivity, can also be visually inspected. Tissues with impeded diffusion appear hypointense on ADC maps/images, while they remain hyperintense on DWI. However, "T2 shine through" effect will result in a hyperintense signal in a tissue on both DWI as well as ADC maps. T2 shine through errors can also be reduced using a short TE and large *b* value, in addition to inspecting the ADC map[1].

QUANTITATIVE ANALYSIS OF DWI

The logarithm of relative signal intensity of tissue (signal decay) on the y-axis against the *b* values on the x-axis results in a line (exponential function). The slope of this line represents the ADC. ADC is a quantitative measure of tissue diffusivity and is expressed in ($\times 10^{-3}$) as mm^2/s. This graphical fit can be improved by using multiple *b* values to reduce error involved in the calculation and monoexponential and multiexponential modeling of signal decay. ADC maps of the entire imaged volume can be generated automatically on most MRI scanners and workstations. Average ADC value is determined by drawing an electronic region of interest (ROI) on an ADC map image generated on the scanner. Decreased ADC values compared to normal tissue indicate restricted (or impeded) diffusion[3]. Conversely, increased ADC values suggest increased diffusivity. Quantitative analysis has advantages over visual qualitative analysis in that it is independent of magnetic field strength and can overcome the effects of "T2 shine-through"[1]. A simple method to detect T2 shine-through is to use the "exponential image" formula, where an increased signal ratio [DWI signal intensity (at $b = X$)/unweighted signal intensity (at $b = 0$)] suggests true restricted diffusion[1]. The ADC is calculated for each pixel and displayed as a

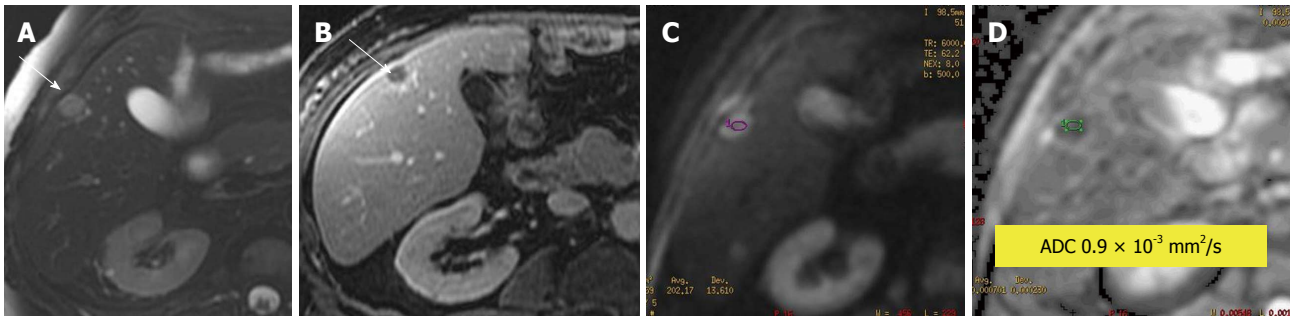

Figure 1 Leiomyosarcoma metastasis to liver. A: Axial fat-suppressed, T2-weighted (T2W) Fast Spin-Echo image; B: Post contrast T1-weighted gradient recalled-echo image; C: Diffusion-weighted imaging; D: Apparent diffusion coefficient (ADC) map. The T2W hyperintense and rim-enhancing lesion is a pathologically established metastasis (arrow) with an ADC value of 0.9 × 10^{-3} mm^2/s, indicating impeded diffusion likely due to its highly cellular nature.

parametric map. An average ADC value can be obtained by drawing an electronic ROI, as mentioned above. Certain tissue characteristics, such as increased cellularity and ischemia, are known to be associated with low ADC values due to restricted (or impeded) diffusion of water[1].

CLINICAL APPLICATIONS

Computed tomography (CT) and conventional MRI are relatively insensitive to early treatment changes in the setting of malignancy. Common imaging biomarkers that suggest response to therapy, such as decreased tumor size and change in Hounsfield unit attenuation, often take weeks to months to become evident. DWI has been shown to be sensitive to the microenvironmental changes in tumors at the molecular level that result from treatment and, thus, may be able to predict early tumor response to chemotherapy or radiotherapy[3]. Specifically, this technique may be able to detect disintegration of the cell membrane with tumor lysis and increased extracellular space, resulting in increased diffusion of water and increased ADC values compared to pre-treatment values[1,7,8]. However, increased vascularity with associated increased perfusion, which may be significant in some tumors, also affects the DWI characteristics[1,9]. Therapies directed against the tumor vasculature may result in reduced ADC values, especially when DWI is performed using low *b* values, which are sensitive to vascular perfusion effects[1,10]. Within the first 24 h after initiating treatment, treatment effects may be observed due to cell swelling, with a resulting transient decrease in ADC value[1,10]. Tumors with low pretreatment ADC values have a tendency to respond better to chemotherapy and radiation therapy (*e.g.*, colorectal carcinoma liver metastases[11] and rectal carcinoma[12,13]. Tumors with high pretreatment ADC values are likely to be more necrotic than those with low ADC values and these have diminished sensitivity to chemotherapy and radiation therapy as they are often poorly perfused and contain hypoxic and acidotic areas[1,11-13]. Increased ADC values (within 1 wk post-therapy) have been shown to precede the reduced tumor size[1,11-13].

DWI has also demonstrated the ability to detect recurrent disease earlier than conventional MRI and CT imaging[3]. DWI appears to be a useful adjunct for the detection of metastatic sites of neoplasm, including otherwise subtle and difficult to detect lesions on routine abdomen MRI examinations, both at the time of initial diagnosis and at follow-up after treatment as mentioned below in a separate section[3].

Liver

Regarding DWI of the liver, *b* values of 0-500 are usually adequate. Susceptibility artifact from gas within the stomach and colon and cardiac and respiratory motion artifacts are potential challenges to be overcome.

Tumors may impede diffusion because they are frequently hypercellular compared with the surrounding tissue from which they originate, making them appear relatively hyperintense on DWI. Thus, DWI can be useful for detecting liver metastases (Figure 1). In the liver, low *b*-value images ($b \leqslant 150$) suppress high signal from blood flow in hepatic vessels, resulting in "black blood" images that are useful for detecting lesions. Low-*b*-value DWI has been shown to be superior to both fat-suppressed T2-weighted and short tau inversion recovery (STIR) images in detecting focal liver lesions; this is especially true for metastatic lesions < 1 cm in size[4]. Nasu *et al*[14] found DWI to be more accurate than superparamagnetic iron oxide-enhanced MRI for detecting liver metastases. In fact, no significant difference existed in the performance of DWI compared with that of gadolinium-enhanced T1-weighted images on a per-lesion basis[4,14]. Many times, DWI actually increases the conspicuity of the lesions and may detect more lesions than seen on other pulse sequences (Figure 2). Hence, DWI may be a useful alternative sequence in patients with a contraindication to gadolinium.

A qualitative (visual) assessment can distinguish between solid and cystic liver tumors but cannot differentiate among different types of solid lesions (Figures 1-7). Quantitative assessment of ADC values can differentiate some benign lesions (*e.g.*, cysts and most hemangiomas) which have high ADC values (Figures 6 and 7) from certain malignant lesions [*e.g.*, hepatocellular carcinoma (HCC) and metastases] which have low ADC values (Figures 1 and 4)[15].

ADC values in hepatic abscesses are generally lower than those in cystic and necrotic metastases, with reported mean ADC values of 0.67 ± 0.35 × 10^{-3} mm^2/s in hepatic

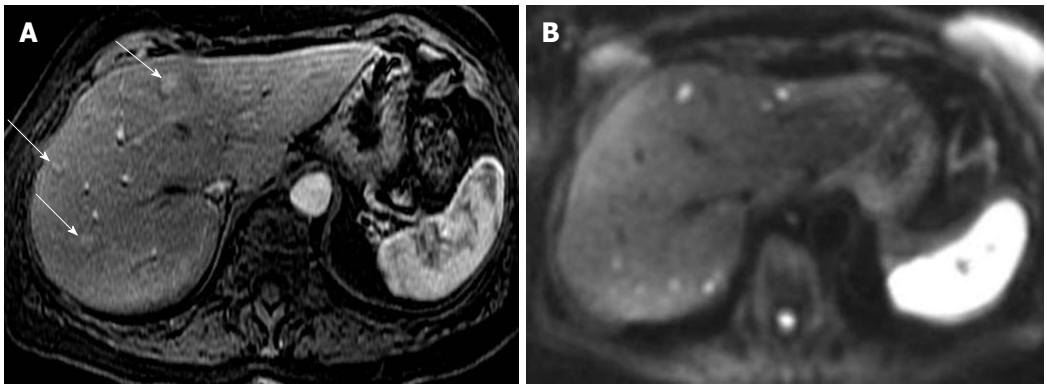

Figure 2 Neuroendocrine metastases to liver. A: Axial arterial phase post contrast T1-weighted (T1W) gradient recalled-echo; B: Diffusion-weighted image (DWI). Only 3 enhancing metastatic lesions are seen on the post contrast T1W image. DWI increases conspicuity of these lesions and also shows many more bilobar high signal metastatic lesions with impeded diffusion.

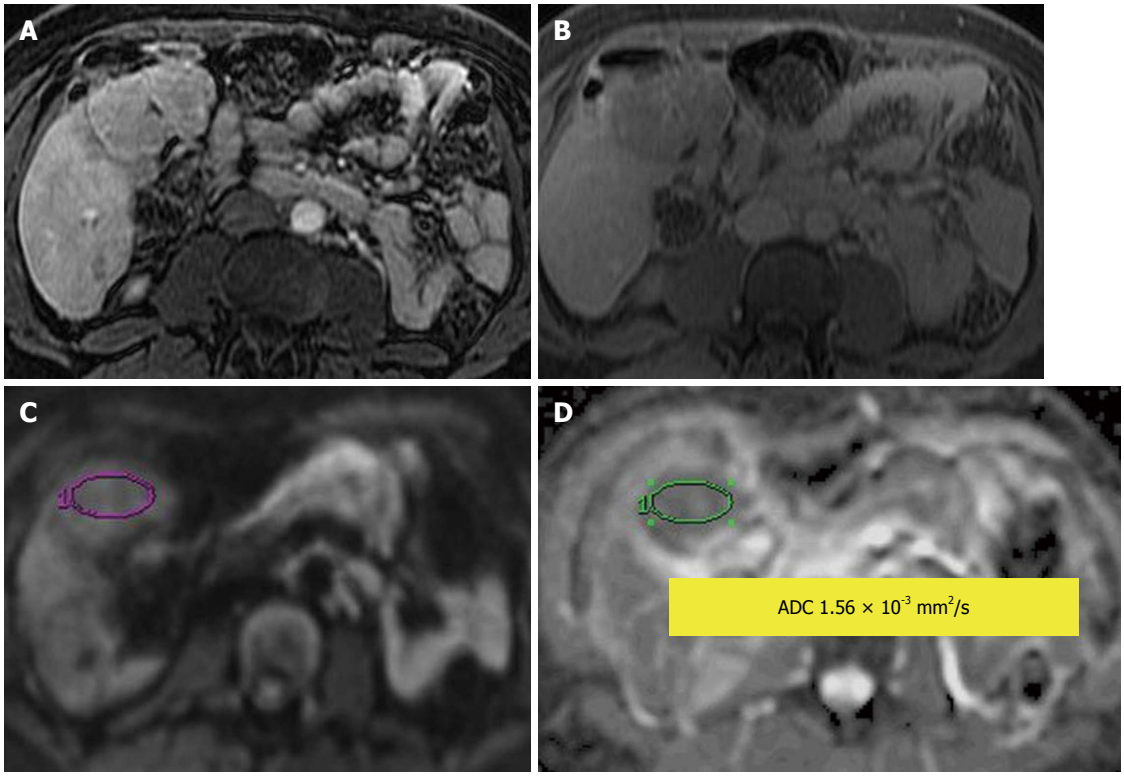

Figure 3 Hepatocellular adenoma. A: Contrast-enhanced T1-weighted gradient recalled-echo in arterial phase; B: Delayed post contrast phase; C: Diffusion-weighted image; D: Apparent diffusion coefficient (ADC) map. An arterial enhancing lesion with delayed wash out is visible; it demonstrates impeded diffusion with ADC = 1.56 × 10^{-3} mm^2/s.

abscesses, 2.65 ± 0.49 × 10^{-3} mm^2/s in cystic and necrotic tumors, compared to mean ADC value of 1.98 ± 0.37 × 10^{-3} mm^2/s in normal liver parenchyma[16]. Consequently, abscesses and some inflammatory lesions may mimic malignancy, based upon low ADC values and/or impeded diffusion (Figure 8).

Considerable overlap (Figures 1-5 and 7) also exists in the ADC values of solid benign and malignant hepatic lesions. An increasing number of studies have evaluated the use of quantitative ADC measurements in liver lesions, but discrepancies in scan parameters lead to discrepancies in reported ADC values[3,17]. Hence, radiologists must interpret DWI in conjunction with other MRI pulse sequences, especially keeping in mind the pretest probability of an abnormality[3,4,18-20]. Overall, the limitation of the DWI sequence is predominantly lesion characterization rather than lesion detection. Although it has a significantly high overall detection rate for liver metastases, with excellent conspicuity, detection of left lobe lesions may be difficult because of image-degrading cardiac motion artifacts[3,21,22].

Lower pretreatment ADC values have been shown to be predictive of a good response to treatment in cases of liver metastases from colorectal and gastric origins[3,11,13].

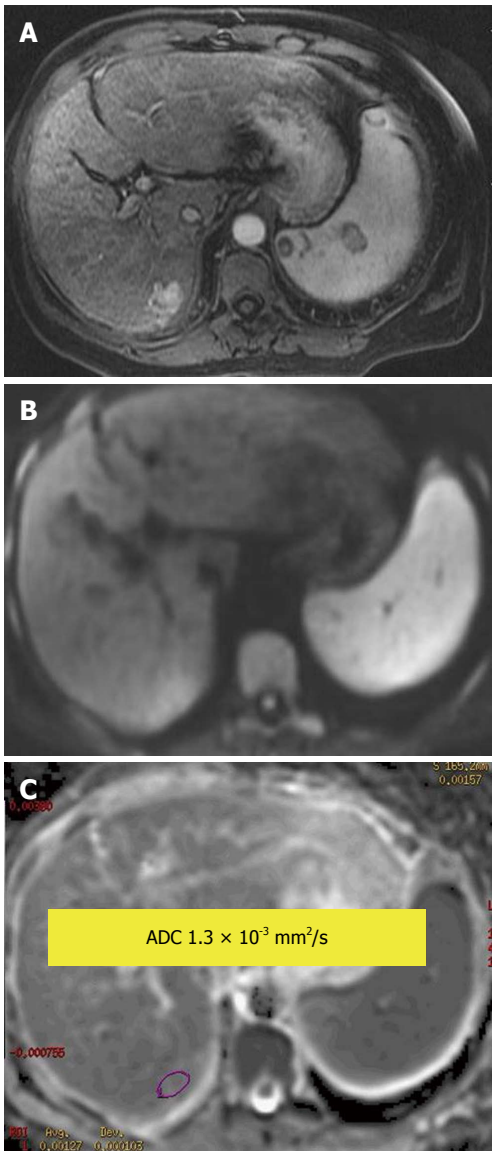

Figure 4 Hepatocellular carcinoma. A: Enhanced arterial phase T1-weighted gradient recalled-echo; B: Diffusion-weighted image; C: Apparent diffusion coefficient (ADC) map. An arterial enhancing lesion with impeded diffusion and ADC = 1.3 × 10^{-3} mm^2/s is visible.

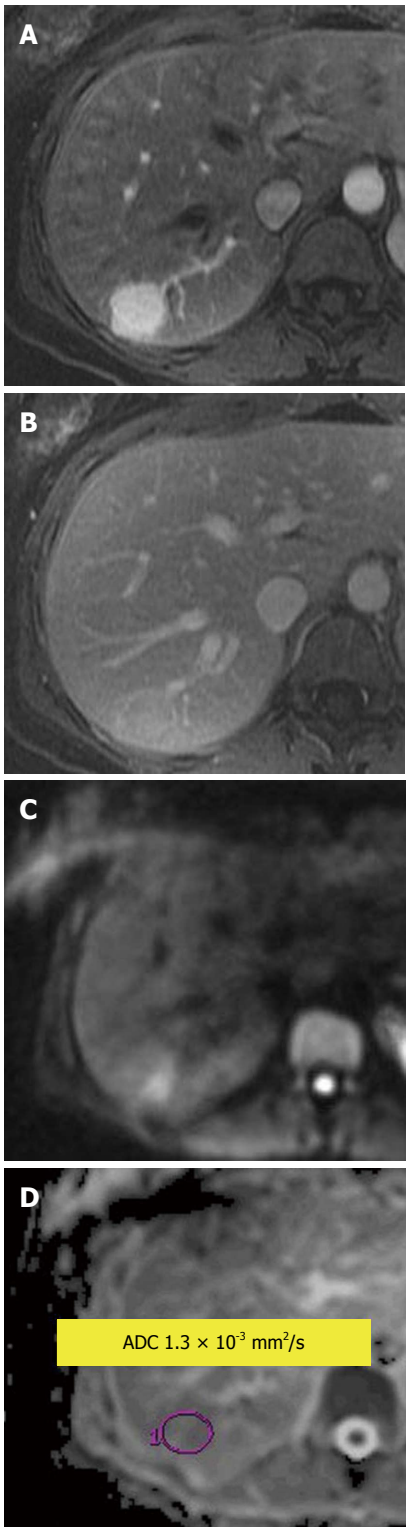

Figure 5 Focal nodular hyperplasia. A: Enhanced arterial phase; B: Venous phase T1-weighted gradient recalled-echo; C: Diffusion-weighted image; D: Apparent diffusion coefficient map (ADC). An arterial enhancing lesion which becomes isointense to slightly hyperintense to liver on venous phase and shows impeded diffusion with ADC of 1.3 × 10^{-3} mm^2/s.

High pretreatment ADC values may indicate poorly perfused necrotic regions in tumors, with the resulting poor delivery of chemotherapeutic agents to these areas[1,3,11]. Responding tumors show an increase in ADC values after treatment, whereas non-responding tumors and liver parenchyma show minimal change[3].

DWI may also be useful for assessing treatment response of HCC to locoregional therapies, such as radiofrequency ablation and chemoembolization[3,23]. Suspected areas of residual or recurrent tumor at ablation sites are usually seen as hyperintense foci on DWI, while the necrotic areas appear hypointense[3,23] (Figure 9). Recurrent tumors at the ablation site have been shown to have lower ADCs than the adjacent ablation zone and background normal liver parenchyma[3,23]. On the other hand, wide variability has been observed in ADC values (although higher than pretreatment value) of tumors after transarterial chemoembolization (TACE)[3,24,25]. After TACE, perilesional inflammation and arterial reperfusion of the perilesional atrophic area may lead to false positive ADCs,

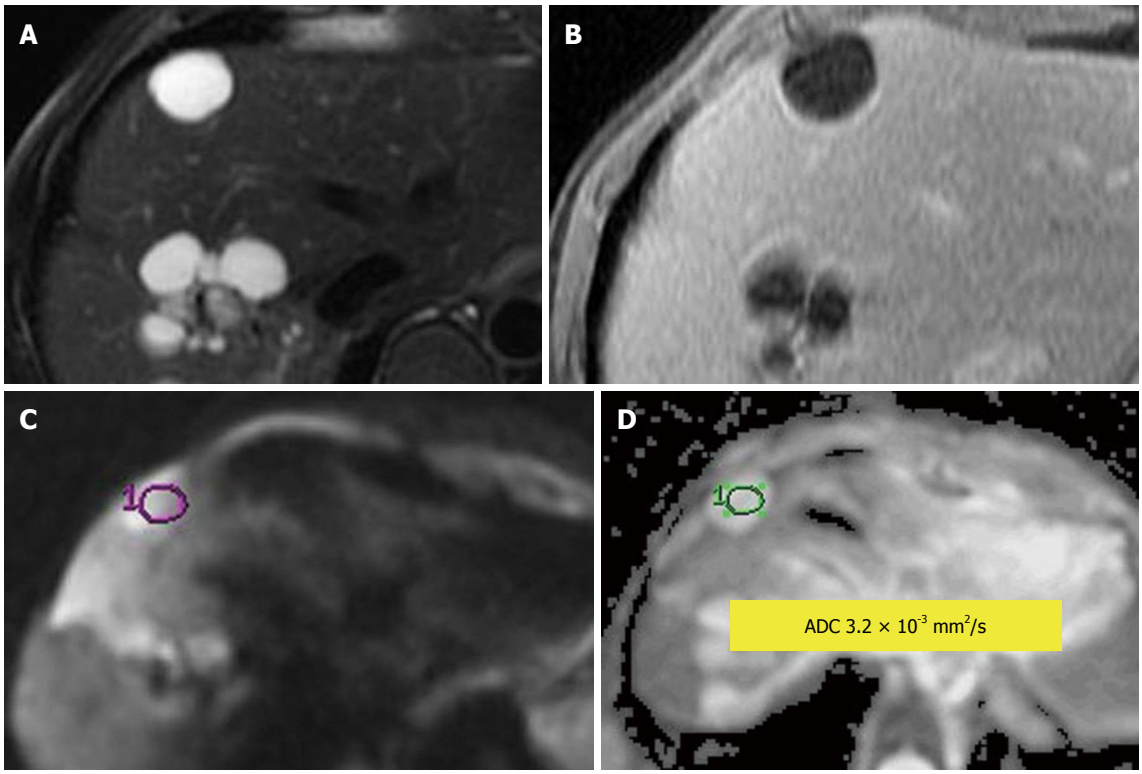

Figure 6 Simple hepatic cyst. A: Fat-suppressed T2-weighted (T2W) Fast Spin-Echo; B: Enhanced T1-weighted gradient recalled-echo; C: Diffusion-weighted image; D: Apparent diffusion coefficient (ADC) map. A T2W hyperintense non-enhancing lesion consistent with a simple cyst with ADC = 3.2 × 10^{-3} mm^2/s. No impeded diffusion is visible.

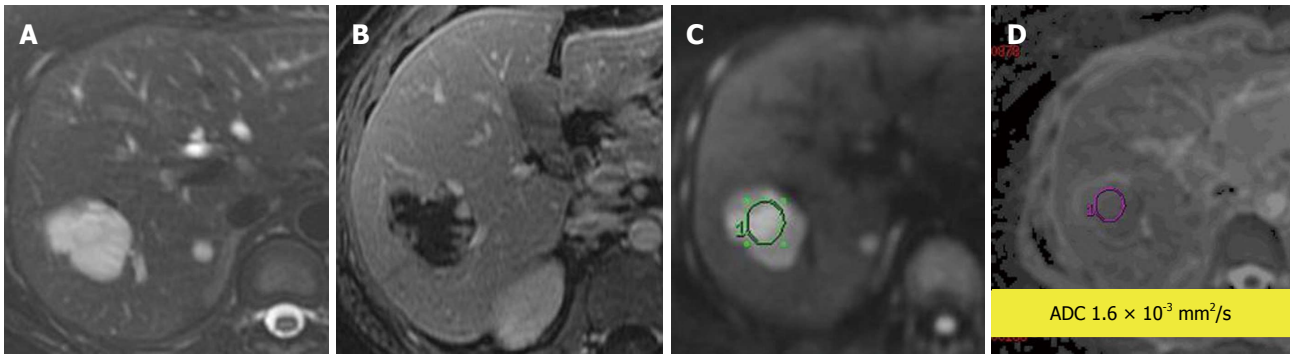

Figure 7 Cavernous hemangioma in the liver. A: Fat-suppressed T2-weighted (T2W) Fast Spin-Echo; B: Enhanced (arterial phase) T1-weighted gradient recalled-echo; C: Diffusion-weighted image; D: Apparent diffusion coefficient map (ADC) map. A cavernous hemangioma with a typical T2W hyperintense signal and enhancement (peripheral discontinuous on arterial post contrast phase) characteristics and ADC = 1.6 × 10^{-3} mm^2/s.

suggesting false tumor recurrence and hence affecting the accuracy of conventional MRI[3,24,25]. In cases of HCCs treated with angiogenesis-inhibiting agents, contrary results have been described than those expected, *i.e.*, ADC values decrease rather than increase after treatment. This is likely due to ischemia and hemorrhage in the tumor, which can be associated with these agents[3,23]. In these cases, lower ADC values at 3 mo post-treatment have been shown to correlate well with HCC progression, as expected[3,23].

In diffuse hepatic diseases, chronic hepatitis and cirrhosis, lower ADCs are more often found in the liver parenchyma than in healthy livers[4] (Figure 10). In fact, the ADC values of cirrhotic livers can overlap with the ADC values of malignant liver lesions, affecting the reliability of DWI. Low ADC values are also seen in cases of nonalcoholic fatty disease and hepatic fibrosis. ADCs have been shown to be useful for differentiating severe hepatic fibrosis from mild or moderate fibrosis[4]. However, considerable overlap has been observed in ADC values, with varying degrees of fibrosis, inflammation and fatty changes; hence, DWI is still ancillary[4].

Biliary tree

Gallbladder and biliary ducts have similar DWI features and ADCs to those of simple cysts because of their content. Few studies have been performed of DWI of

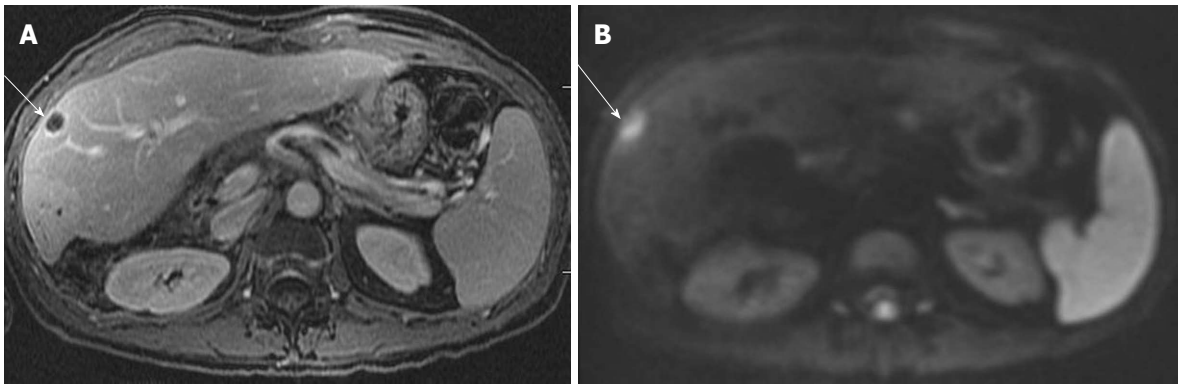

Figure 8 Liver abscess in a patient with Crohn disease. A: Axial post contrast T1-weighted gradient recalled-echo; B: Diffusion-weighted image image. Rim enhancing lesion is seen in the right hepatic lobe, with corresponding bright lesion on diffusion weighted image. The apparent diffusion coefficient map (not shown) showed corresponding hypointense lesion suggesting true impeded diffusion. This should not be confused with liver tumors which may also show impeded diffusion. Appropriate clinical settings should suggest the diagnosis. The lesion resolved with antibiotics on follow-up.

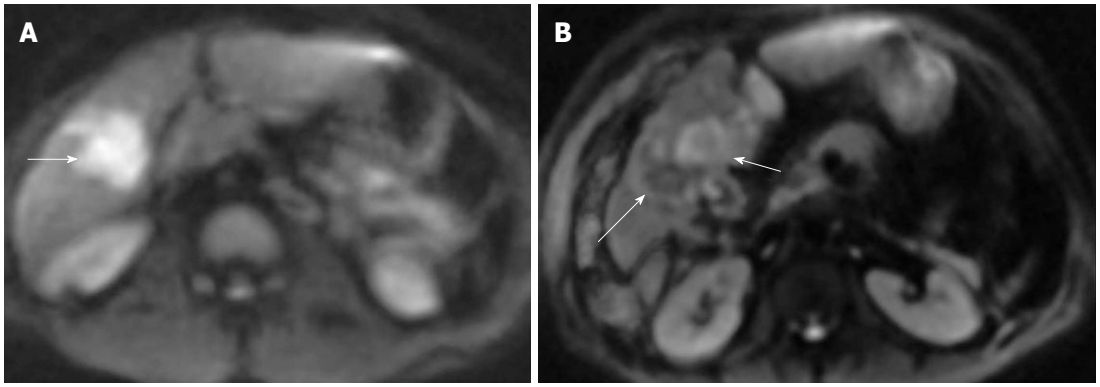

Figure 9 Hepatocellular carcinoma (arrows) on diffusion-weighted image (A) before and (B) after transarterial chemoembolization. A: Hepatocellular carcinoma (HCC) was hyperintense compared with the cirrhotic liver on diffusion weighted image, with an apparent diffusion coefficient (ADC) = 1.41 × 10^{-3} mm^2/s *vs* 1.08 × 10^{-3} mm^2/s for the liver; B: After transarterial chemoembolization, HCC showed a residual area of hyperintense signal (short arrow) with ADC = 1.38 × 10^{-3} mm^2/s (residual tumor) and a new area of hypointense signal (long arrow) with ADC = 1.87 × 10^{-3} mm^2/s (coagulation necrosis), indicating a partial response. This finding of necrosis was supported by lack of enhancement on gadolinium-enhanced imaging and confirmed on follow-up studies.

the biliary tree. Sugita *et al*[26] found lower ADC values in gallbladder carcinoma, with a mean of 1.28 ± 0.41 × 10^{-3} mm^2/s, than in control lesions, such as chronic cholecystitis, adenomyomatosis and polyps, which have a mean ADC of 1.92 ± 0.21 × 10^{-3} mm^2/s. Cui *et al*[27] found that DWI has high diagnostic accuracy for detecting extrahepatic cholangiocarcinoma and DWI helped correctly diagnose cases of cholangitis and biliary stones from extrahepatic cholangiocarcinoma in their study[4,26,27]. For bile duct stones, ADC was 0.48 ± 0.22 × 10^{-3} mm^2/s in contrast to ADC of 1.31 ± 0.29 × 10^{-3} mm^2/s in cholangiocarcinoma[27]. Linear hyperintensity can be seen along the intrahepatic portal vein branches in cases of ascending cholangitis, with occasional abscesses also appearing hyperintense. High *b* value DWI may help to differentiate cholangitis which will lose signal, becoming relatively isointense to liver, *vs* the abscesses which will remain hyperintense, when compared to low *b* value DWI[4,26,27].

Pancreas

Normally, the head and body of the pancreas have higher ADC values than the tail. ADC measurements in pancreatic adenocarcinoma (Figure 11) are lower compared to normal pancreas[28-34], with a reported cut-off value of 1.4 × 10^{-3} mm^2/s. ADC values have been shown to be useful for differentiating pancreatic malignancies from normal pancreatic tissue but not for differentiating malignancy from other benign or inflammatory lesions[4,28,29,33]. ADC values have also been used to differentiate between pancreatic adenocarcinoma and mass-forming pancreatitis. Mass-forming pancreatitis has either lower or higher ADC values than that in pancreatic carcinoma, but these follow the ADC values of remaining pancreatic parenchyma. On the contrary, ADC values in a focal pancreatic cancer are invariably lower than that of the rest of the pancreatic parenchyma[33,35]. DWI has been found to be comparable to conventional MRI for detection of neuroendocrine tumors and is particularly superior for detecting small (0.5-1 cm) and non-hypervascular lesions[4,36].

The few studies that have been performed to differentiate among cystic lesions of the pancreas (Figures 12-14) have shown controversial results, with overlapping ADC values between pseudocysts and mucinous neoplasms[4]. Acute pancreatitis has higher ADCs than normal paren-

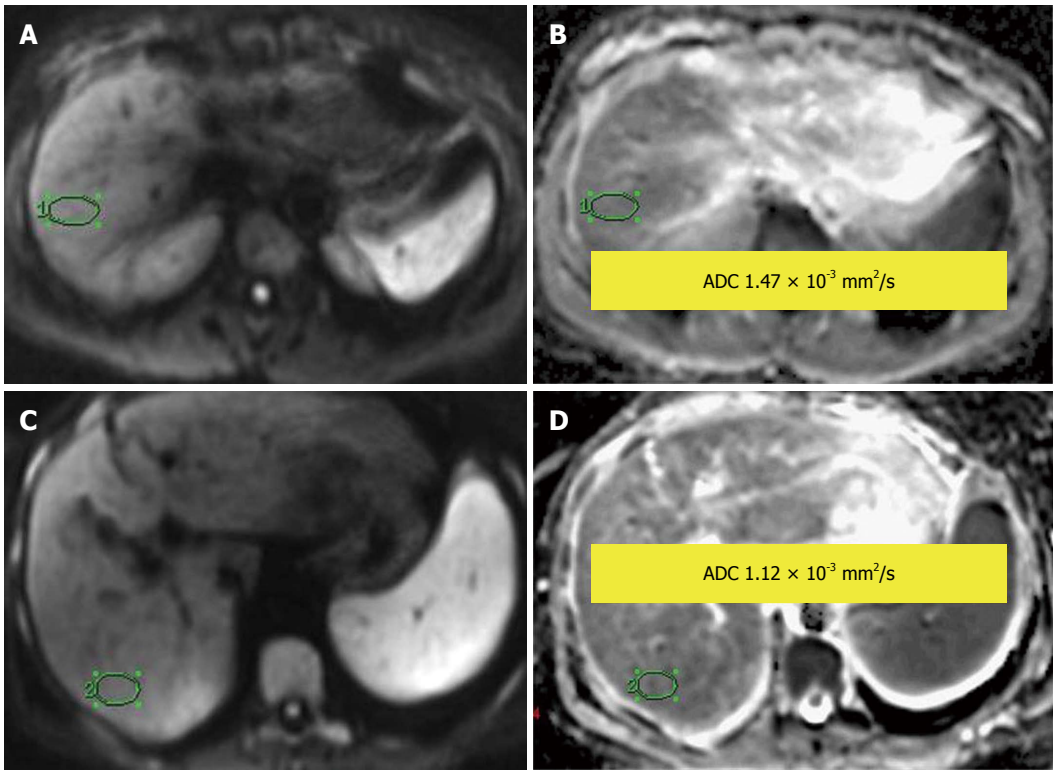

Figure 10 Normal liver parenchyma. A, B: Diffusion-weighted image (DWI) (A) and apparent diffusion coefficient (ADC) map (B), showing ADC = 1.47 × 10^{-3} mm^2/s; Liver cirrhosis: (C) DWI and (D) ADC map, showing ADC = 1.12 × 10^{-3} mm^2/s.

chyma because of the increased diffusion of water that results from increased vascular permeability and edema[37]. Chronic pancreatitis has lower ADC values because of fibrosis and reduced exocrine function[37]. Autoimmune pancreatitis has lower ADCs than acute or chronic pancreatitis. These values can also be monitored to assess treatment response during corticosteroid therapy[4,38].

Kidneys

The normal renal cortex has higher ADC values than the medulla. DWI has been found to be useful in assessing diffuse as well as focal renal diseases, including evaluation of renal masses. Solid renal cell carcinomas (RCCs) have significantly lower ADC values (Figure 15) than simple or mildly complex cysts and oncocytomas[39,40]. Taouli *et al*[39] were able to differentiate between oncocytomas and RCC using an ADC cut-off of 1.66 × 10^{-3} mm^2/s. Renal cysts have considerably higher ADCs than solid renal masses[39,40]. ADC values of renal cysts vary with internal cyst contents. For example, proteinaceous or hemorrhagic contents may have lower ADC values than simple cysts[4]. Cystic RCCs and benign hemorrhagic cysts may have overlapping ADC values and thus may not be differentiated. However, the ADC values in the solid portion of necrotic or cystic RCCs are usually lower. Abscesses show markedly impeded diffusion and decreased ADC values, as expected[39,40]. Non-clear cell RCCs usually have lower ADC values than clear cell RCCs[41]. This may be due to decreased perfusion in papillary (non-clear cell) RCCs, which are typically hypovascular compared with clear cell carcinomas. Angiomyolipomas have been shown to have lower ADC values than other renal masses, possibly because the muscle and fat components restrict diffusion[39,40].

ADC values may also be useful for functionally assessing the kidneys, as reported in several studies. Lower ADC values of the renal parenchyma have been observed in acute and chronic renal failure, with the lowest ADC values in patients with chronic renal failure[42,43]. A relationship between ADC value and serum creatinine values was found in these cases. However, no relationship has been observed between ADCs and glomerular filtration rate. Low ADC values due to impeded diffusion have also been found in the affected portions of kidneys in pyelonephritis[4] and significantly lower ADC values s have been found in the kidneys of patients with renal arterial stenosis than in those of patients with normal renal arteries[44]. Similarly, significantly lower ADC values have been observed in the renal collecting systems of individuals with pyonephrosis when compared to uncomplicated hydronephrosis[45,46]. Hydronephrotic kidneys with moderate and severe decrease in renal function have much lower ADCs than hydronephrotic kidneys with normal function[45,46].

Adrenal glands

Normal adrenal glands have a high signal (hyperintense) on DWI with non-pathological impeded diffusion. Although pheochromocytomas have relatively higher ADC values than adrenocortical adenomas and malignancies[47],

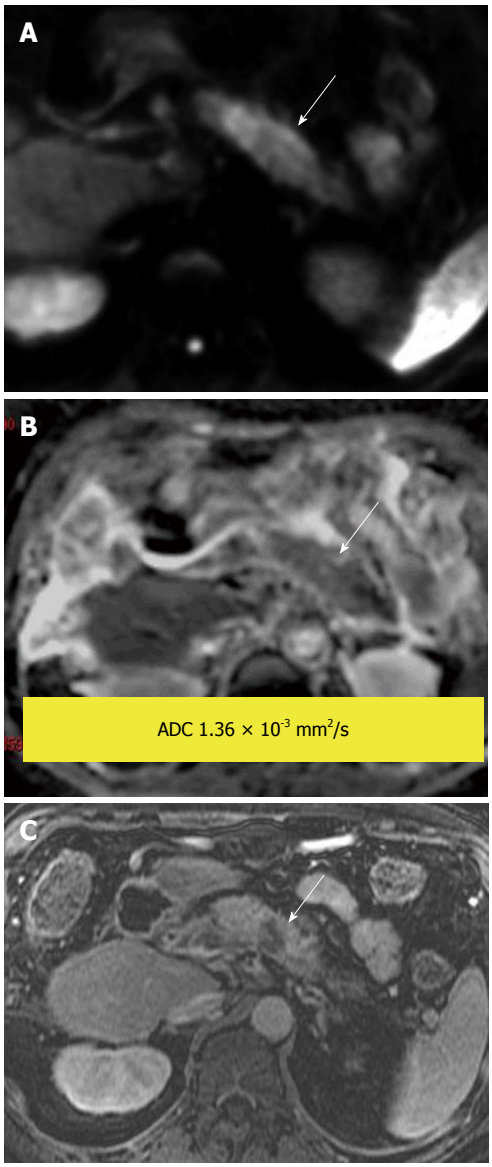

Figure 11 Pancreatic ductal adenocarcinoma. Hyperintense mass demonstrated on (A) diffusion-weighted image due to impeded diffusion, confirmed by a hypointense signal on (B) apparent diffusion coefficient map. Findings are supported by a (C) post-gadolinium T1-weighted image that shows the tumor to be hypo enhancing compared with the enhancing pancreatic parenchyma.

no diagnostic utility has been found for DWI/ADC values in differentiating between lipid-rich and lipid-poor adenomas and between benign and malignant nodules (or masses) (Figure 16). Cysts have higher ADC values than almost all other adrenal lesions, as generally expected[47,48].

Spleen

Normal spleen, as well as accessory spleens and splenules, have the greatest degree of nonpathological impeded diffusion of all solid abdominal organs. Significantly elevated splenic ADC values may be observed in individuals with cirrhosis[4]. Ertan *et al*[49] suggested that higher ADC values in an enhancing splenic lesion indicates a vascular etiology. To our knowledge, no other data exist regarding DWI of splenic lesions[4,49].

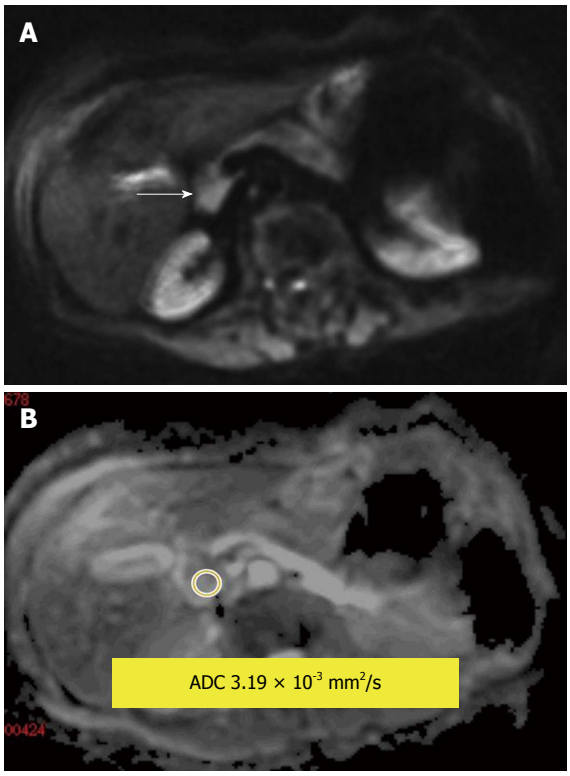

Figure 12 Serous cystadenoma in the pancreatic head. A: Diffusion-weighted image; B: Apparent diffusion coefficient (ADC) map. Measured lesion ADC = 3.19 × 10^{-3} mm^2/s. The internal reference can be used; the reference for the fluid in this study (cerebrospinal fluid) was ADC = 3.78 × 10^{-3} mm^2/s.

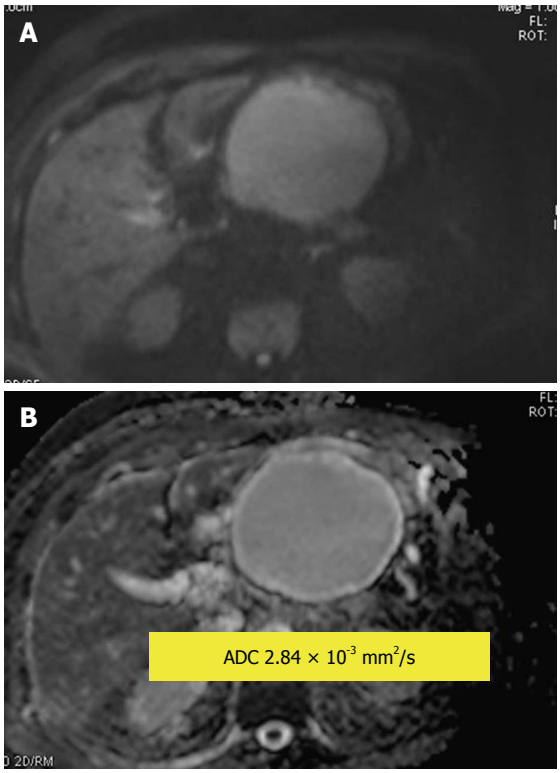

Figure 13 Pancreatic pseudocyst. A: Diffusion-weighted image (DWI); B: Apparent diffusion coefficient (ADC) map. Hyperintensity of the cyst on DWI is due to the T2 shine through effect. Measured lesion ADC = 2.84 × 10^{-3} mm^2/s. The reference for the fluid in this study (cerebrospinal fluid) was ADC = 4.06 × 10^{-3} mm^2/s.

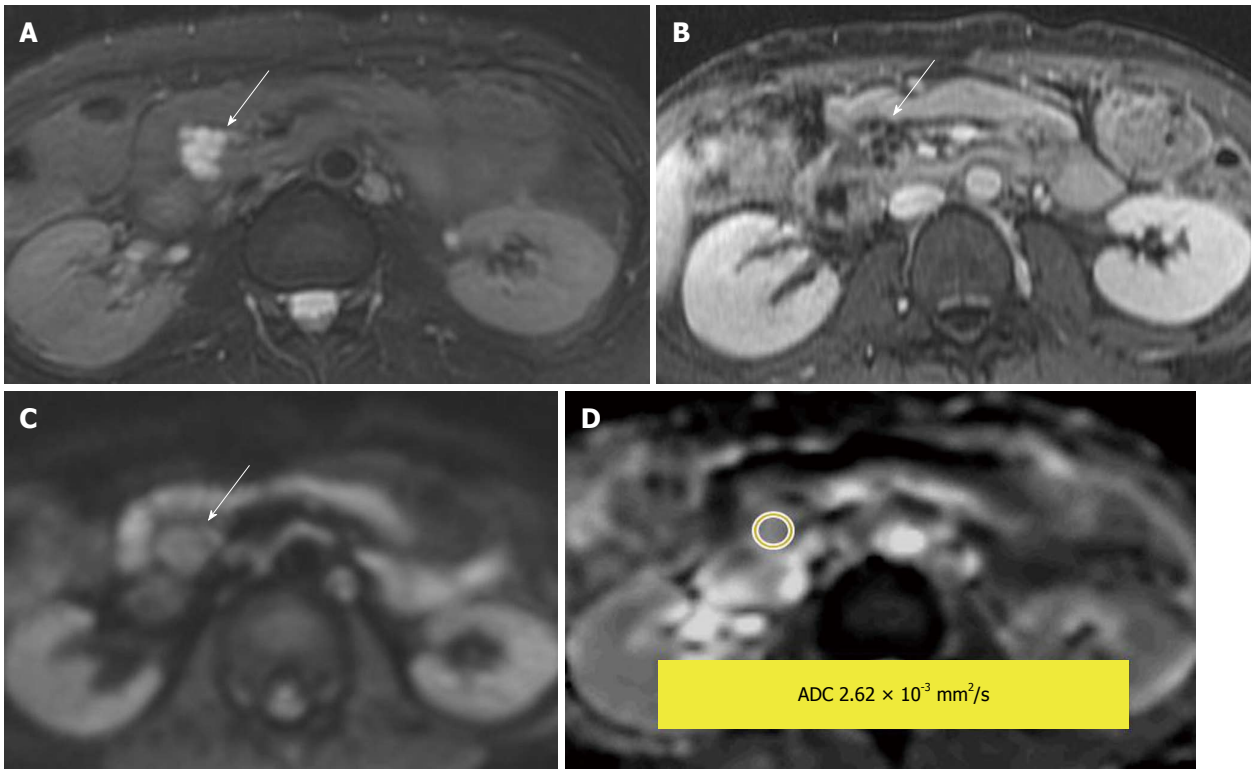

Figure 14 Side branch intraductal papillary mucinous neoplasms. A: Fat-saturated T2-weighted (T2W) Fast Spin-Echo; B: Post contrast T1-weighted gradient recalled-echo; C: Diffusion-weighted image; D: Apparent diffusion coefficient (ADC) map. A lobulated T2W hyperintense lesion with enhancement of the rim and internal septae. The measured lesion ADC = 2.62 × 10^{-3} mm^2/s. The reference for fluid in this study (cerebrospinal fluid) was ADC = 3.36 × 10^{-3} mm^2/s.

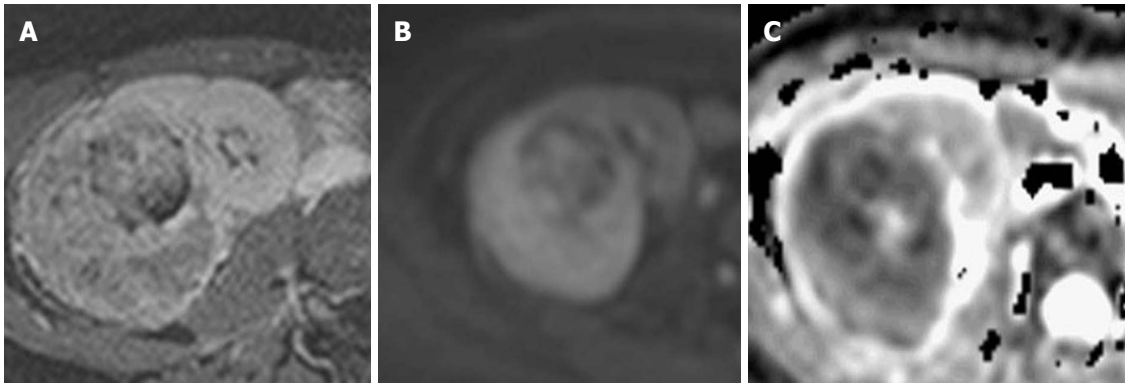

Figure 15 Renal cell carcinoma. (A) Heterogeneously enhancing mass on post contrast T1-weighted gradient recalled-echo image, demonstrating a high signal on (B) diffusion-weighted image and a low signal on (C) apparent diffusion coefficient, indicating impeded diffusion.

Vascular thrombosis

Deep venous thrombosis is a relatively common and potentially life-threatening condition that accounts for almost all cases of pulmonary thromboembolism. Deep venous thrombosis has a multitude of causes, although most episodes relate to abnormal veins and venous stasis (*e.g.*, due to varicose veins and associated venous insufficiency). Acute-subacute deep venous thrombi may demonstrate abnormal signal hyperintensity, similar to that observed in cerebral venous thrombosis[50].

Whole-body DWI

STIR EPI DWI with a *b* value of 1000 mm^2/s can be useful for evaluating lymphadenopathy in patients with lymphoma and other cancers as highly cellular lymph nodes can be seen well as foci of hyperintense signal on DWI. However, because DWI detects abnormalities on the basis of tissue cellularity, not all detected abnormalities are necessarily malignant as normal lymph nodes or some benign lesions are also cellular, impeding diffusion[1,51]. Small and otherwise difficult to visualize abdominopelvic tumors involving peritoneal, omental and mesenteric surfaces may also be well visualized on DWI because of impeded diffusion, resulting in high signal on DWI against suppressed background signal (Figure 17)[1,51]. Whole-body DWI may also be useful for staging a variety of malignant tumors[52].

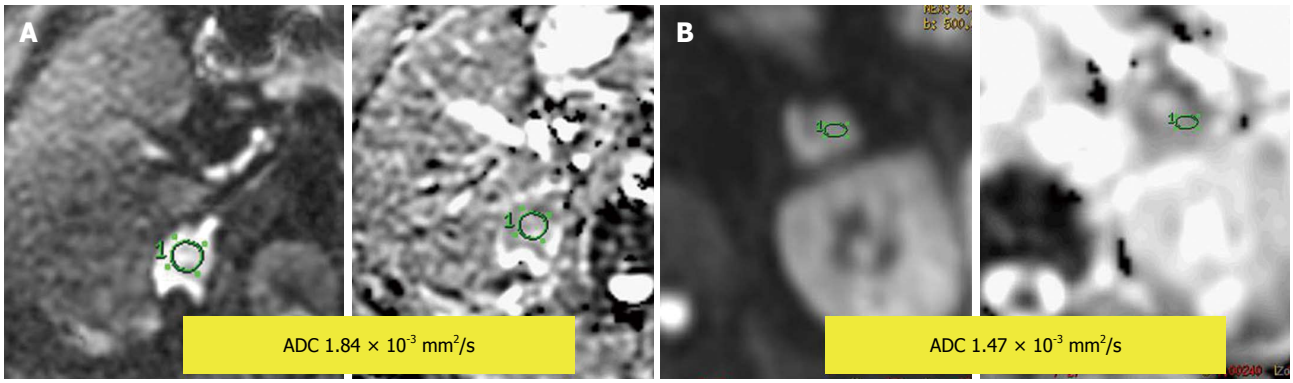

Figure 16 Diffusion-weighted image and apparent diffusion coefficient map. A: An adrenal mass with impeded diffusion and apparent diffusion coefficient (ADC) = 1.84 × 10^{-3} mm^2/s; B: An adrenal mass with impeded diffusion and ADC = 1.47 × 10^{-3} mm^2/s.

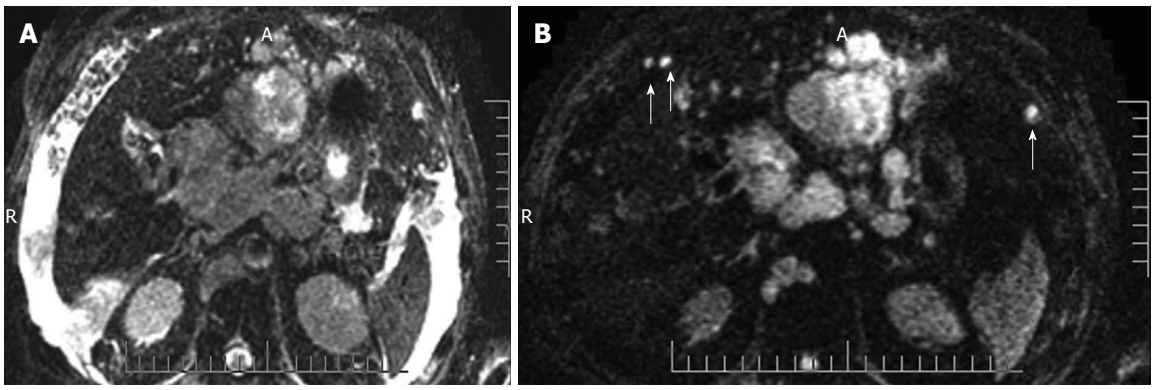

Figure 17 Peritoneal metastases on diffusion-weighted image. A: Due to ascites, peritoneal nodules are not well seen on b = 0 sequence of diffusion-weighted image; B: But, on b = 500, all the ascites is suppressed and peritoneal nodules/metastases become conspicious (arrows).

It is possible that whole-body DWI could perform similarly to positron emission tomography imaging, although further research is needed to determine its utility.

LIMITATIONS

The limitations of DWI include both low SNR and spatial resolution due to hardware limitations. High bandwidth, EPI sequences and motion artifacts related to respiratory, cardiac and voluntary movements are also limitations. Breath hold scans with respiratory and electrocardiographic triggering can be used to minimize motion related artifacts, although these techniques prolong image acquisition time. Susceptibility artifacts due to magnetic field inhomogeneity, the presence of certain metals and air-tissue and water-fat interfaces can also substantially degrade image quality. Eddy currents due to switching gradients may lead to geometric distortion and image-shearing artifacts[3,53-55].

CHALLENGES AND SCOPE

The current lack of standardization with respect to technical parameters utilized, such as pulse sequence type, TR, TE, *b* values utilized, gradient direction and modeling method of signal decay, are major challenges to the reproducibility and reliability of abdominal DWI and measured ADC values. Such differences in technique can result in substantial differences in measured ADC values, even for similar disease states. DWI software also needs continued refinement in order to reduce image noise and for assessing fractional anisotropy and perfusion fraction. As the ADC values of certain tumors appear to increase with treatment and may decrease over time, optimum imaging time is essential to avoid interpretation errors that could adversely affect patient management and outcomes[1,3,4,17].

CONCLUSION

DWI undoubtedly has valuable applications in the abdomen, such as detection of a variety of lesions and evaluating tumor response to treatment. However, its use in many other medical conditions remains controversial and/or unknown. Extensive research into this form of functional imaging is needed to standardize technical parameters and optimize image quality. Additional research will also be necessary to determine DWI's role as a problem-solving tool in various abdominal applications.

REFERENCES

1 **Koh DM**, Collins DJ. Diffusion-weighted MRI in the body:

applications and challenges in oncology. *AJR Am J Roentgenol* 2007; **188**: 1622-1635 [PMID: 17515386 DOI: 10.2214/AJR.06.1403]
2 **Kwee TC**, Takahara T, Ochiai R, Nievelstein RA, Luijten PR. Diffusion-weighted whole-body imaging with background body signal suppression (DWIBS): features and potential applications in oncology. *Eur Radiol* 2008; **18**: 1937-1952 [PMID: 18446344 DOI: 10.1007/s00330-008-0968-z]
3 **Kele PG**, van der Jagt EJ. Diffusion weighted imaging in the liver. *World J Gastroenterol* 2010; **16**: 1567-1576 [PMID: 20355235]
4 **Bittencourt LK**, Matos C, Coutinho AC. Diffusion-weighted magnetic resonance imaging in the upper abdomen: technical issues and clinical applications. *Magn Reson Imaging Clin N Am* 2011; **19**: 111-131 [PMID: 21129638 DOI: 10.1016/j.mric.2010.09.002]
5 **Charles-Edwards EM**, deSouza NM. Diffusion-weighted magnetic resonance imaging and its application to cancer. *Cancer Imaging* 2006; **6**: 135-143 [PMID: 17015238 DOI: 10.1102/1470-7330.2006.0021]
6 **Thoeny HC**, De Keyzer F. Extracranial applications of diffusion-weighted magnetic resonance imaging. *Eur Radiol* 2007; **17**: 1385-1393 [PMID: 17206421 DOI: 10.1007/s00330-006-0547-0]
7 **Moffat BA**, Chenevert TL, Lawrence TS, Meyer CR, Johnson TD, Dong Q, Tsien C, Mukherji S, Quint DJ, Gebarski SS, Robertson PL, Junck LR, Rehemtulla A, Ross BD. Functional diffusion map: a noninvasive MRI biomarker for early stratification of clinical brain tumor response. *Proc Natl Acad Sci USA* 2005; **102**: 5524-5529 [PMID: 15805192 DOI: 10.1073/pnas.0501532102]
8 **Moffat BA**, Hall DE, Stojanovska J, McConville PJ, Moody JB, Chenevert TL, Rehemtulla A, Ross BD. Diffusion imaging for evaluation of tumor therapies in preclinical animal models. *MAGMA* 2004; **17**: 249-259 [PMID: 15580371 DOI: 10.1007/s10334-004-0079-z]
9 **van Rijswijk CS**, Kunz P, Hogendoorn PC, Taminiau AH, Doornbos J, Bloem JL. Diffusion-weighted MRI in the characterization of soft-tissue tumors. *J Magn Reson Imaging* 2002; **15**: 302-307 [PMID: 11891975]
10 **Thoeny HC**, De Keyzer F, Chen F, Ni Y, Landuyt W, Verbeken EK, Bosmans H, Marchal G, Hermans R. Diffusion-weighted MR imaging in monitoring the effect of a vascular targeting agent on rhabdomyosarcoma in rats. *Radiology* 2005; **234**: 756-764 [PMID: 15734932 DOI: 10.1148/radiol.2343031721]
11 **Koh DM**, Scurr E, Collins D, Kanber B, Norman A, Leach MO, Husband JE. Predicting response of colorectal hepatic metastasis: value of pretreatment apparent diffusion coefficients. *AJR Am J Roentgenol* 2007; **188**: 1001-1008 [PMID: 17377036 DOI: 10.2214/AJR.06.0601]
12 **DeVries AF**, Kremser C, Hein PA, Griebel J, Krezcy A, Ofner D, Pfeiffer KP, Lukas P, Judmaier W. Tumor microcirculation and diffusion predict therapy outcome for primary rectal carcinoma. *Int J Radiat Oncol Biol Phys* 2003; **56**: 958-965 [PMID: 12829130]
13 **Dzik-Jurasz A**, Domenig C, George M, Wolber J, Padhani A, Brown G, Doran S. Diffusion MRI for prediction of response of rectal cancer to chemoradiation. *Lancet* 2002; **360**: 307-308 [PMID: 12147376 DOI: 10.1016/S0140-6736(02)09520-X]
14 **Nasu K**, Kuroki Y, Nawano S, Kuroki S, Tsukamoto T, Yamamoto S, Motoori K, Ueda T. Hepatic metastases: diffusion-weighted sensitivity-encoding versus SPIO-enhanced MR imaging. *Radiology* 2006; **239**: 122-130 [PMID: 16493012 DOI: 10.1148/radiol.2383041384]
15 **Taouli B**, Vilgrain V, Dumont E, Daire JL, Fan B, Menu Y. Evaluation of liver diffusion isotropy and characterization of focal hepatic lesions with two single-shot echo-planar MR imaging sequences: prospective study in 66 patients. *Radiology* 2003; **226**: 71-78 [PMID: 12511671]
16 **Chan JH**, Tsui EY, Luk SH, Fung AS, Yuen MK, Szeto ML, Cheung YK, Wong KP. Diffusion-weighted MR imaging of the liver: distinguishing hepatic abscess from cystic or necrotic tumor. *Abdom Imaging* 2001; **26**: 161-165 [PMID: 11178693]
17 **Goshima S**, Kanematsu M, Kondo H, Yokoyama R, Kajita K, Tsuge Y, Watanabe H, Shiratori Y, Onozuka M, Moriyama N. Diffusion-weighted imaging of the liver: optimizing b value for the detection and characterization of benign and malignant hepatic lesions. *J Magn Reson Imaging* 2008; **28**: 691-697 [PMID: 18777553 DOI: 10.1002/jmri.21467]
18 **Sandrasegaran K**, Akisik FM, Lin C, Tahir B, Rajan J, Aisen AM. The value of diffusion-weighted imaging in characterizing focal liver masses. *Acad Radiol* 2009; **16**: 1208-1214 [PMID: 19608435 DOI: 10.1016/j.acra.2009.05.013]
19 **Lichy MP**, Aschoff P, Plathow C, Stemmer A, Horger W, Mueller-Horvat C, Steidle G, Horger M, Schafer J, Eschmann SM, Kiefer B, Claussen CD, Pfannenberg C, Schlemmer HP. Tumor detection by diffusion-weighted MRI and ADC-mapping--initial clinical experiences in comparison to PET-CT. *Invest Radiol* 2007; **42**: 605-613 [PMID: 17700275 DOI: 10.1097/RLI.0b013e31804ffd49]
20 **Vandecaveye V**, De Keyzer F, Verslype C, Op de Beeck K, Komuta M, Topal B, Roebben I, Bielen D, Roskams T, Nevens F, Dymarkowski S. Diffusion-weighted MRI provides additional value to conventional dynamic contrast-enhanced MRI for detection of hepatocellular carcinoma. *Eur Radiol* 2009; **19**: 2456-2466 [PMID: 19440718 DOI: 10.1007/s00330-009-1431-5]
21 **Parikh T**, Drew SJ, Lee VS, Wong S, Hecht EM, Babb JS, Taouli B. Focal liver lesion detection and characterization with diffusion-weighted MR imaging: comparison with standard breath-hold T2-weighted imaging. *Radiology* 2008; **246**: 812-822 [PMID: 18223123 DOI: 10.1148/radiol.2463070432]
22 **Bruegel M**, Rummeny EJ. Hepatic metastases: use of diffusion-weighted echo-planar imaging. *Abdom Imaging* 2010; **35**: 454-461 [PMID: 19471997 DOI: 10.1007/s00261-009-9541-8]
23 **Schraml C**, Schwenzer NF, Martirosian P, Bitzer M, Lauer U, Claussen CD, Horger M. Diffusion-weighted MRI of advanced hepatocellular carcinoma during sorafenib treatment: initial results. *AJR Am J Roentgenol* 2009; **193**: W301-W307 [PMID: 19770299 DOI: 10.2214/AJR.08.2289]
24 **Goshima S**, Kanematsu M, Kondo H, Yokoyama R, Tsuge Y, Shiratori Y, Onozuka M, Moriyama N. Evaluating local hepatocellular carcinoma recurrence post-transcatheter arterial chemoembolization: is diffusion-weighted MRI reliable as an indicator? *J Magn Reson Imaging* 2008; **27**: 834-839 [PMID: 18383261 DOI: 10.1002/jmri.21316]
25 **Yu JS**, Kim JH, Chung JJ, Kim KW. Added value of diffusion-weighted imaging in the MRI assessment of perilesional tumor recurrence after chemoembolization of hepatocellular carcinomas. *J Magn Reson Imaging* 2009; **30**: 153-160 [PMID: 19557734 DOI: 10.1002/jmri.21818]
26 **Sugita R**, Yamazaki T, Furuta A, Itoh K, Fujita N, Takahashi S. High b-value diffusion-weighted MRI for detecting gallbladder carcinoma: preliminary study and results. *Eur Radiol* 2009; **19**: 1794-1798 [PMID: 19190910 DOI: 10.1007/s00330-009-1322-9]
27 **Cui XY**, Chen HW. Role of diffusion-weighted magnetic resonance imaging in the diagnosis of extrahepatic cholangiocarcinoma. *World J Gastroenterol* 2010; **16**: 3196-3201 [PMID: 20593506]
28 **Matsuki M**, Inada Y, Nakai G, Tatsugami F, Tanikake M, Narabayashi I, Masuda D, Arisaka Y, Takaori K, Tanigawa N. Diffusion-weighed MR imaging of pancreatic carcinoma. *Abdom Imaging* 2007; **32**: 481-483 [PMID: 17431713 DOI: 10.1007/s00261-007-9192-6]
29 **Kartalis N**, Lindholm TL, Aspelin P, Permert J, Albiin N. Diffusion-weighted magnetic resonance imaging of pancreas tumours. *Eur Radiol* 2009; **19**: 1981-1990 [PMID: 19308414

DOI: 10.1007/s00330-009-1384-8]
30 **Lee SS**, Byun JH, Park BJ, Park SH, Kim N, Park B, Kim JK, Lee MG. Quantitative analysis of diffusion-weighted magnetic resonance imaging of the pancreas: usefulness in characterizing solid pancreatic masses. *J Magn Reson Imaging* 2008; **28**: 928-936 [PMID: 18821618 DOI: 10.1002/jmri.21508]
31 **Ichikawa T**, Erturk SM, Motosugi U, Sou H, Iino H, Araki T, Fujii H. High-b value diffusion-weighted MRI for detecting pancreatic adenocarcinoma: preliminary results. *AJR Am J Roentgenol* 2007; **188**: 409-414 [PMID: 17242249 DOI: 10.2214/AJR.05.1918]
32 **Ichikawa T**, Haradome H, Hachiya J, Nitatori T, Araki T. Diffusion-weighted MR imaging with single-shot echo-planar imaging in the upper abdomen: preliminary clinical experience in 61 patients. *Abdom Imaging* 1999; **24**: 456-461 [PMID: 10475927]
33 **Fattahi R**, Balci NC, Perman WH, Hsueh EC, Alkaade S, Havlioglu N, Burton FR. Pancreatic diffusion-weighted imaging (DWI): comparison between mass-forming focal pancreatitis (FP), pancreatic cancer (PC), and normal pancreas. *J Magn Reson Imaging* 2009; **29**: 350-356 [PMID: 19161187 DOI: 10.1002/jmri.21651]
34 **Yoshikawa T**, Kawamitsu H, Mitchell DG, Ohno Y, Ku Y, Seo Y, Fujii M, Sugimura K. ADC measurement of abdominal organs and lesions using parallel imaging technique. *AJR Am J Roentgenol* 2006; **187**: 1521-1530 [PMID: 17114546 DOI: 10.2214/AJR.05.0778]
35 **Takeuchi M**, Matsuzaki K, Kubo H, Nishitani H. High-b-value diffusion-weighted magnetic resonance imaging of pancreatic cancer and mass-forming chronic pancreatitis: preliminary results. *Acta Radiol* 2008; **49**: 383-386 [PMID: 18415779 DOI: 10.1080/02841850801895381]
36 **Anaye A**, Mathieu A, Closset J, Bali MA, Metens T, Matos C. Successful preoperative localization of a small pancreatic insulinoma by diffusion-weighted MRI. *JOP* 2009; **10**: 528-531 [PMID: 19734630]
37 **Akisik MF**, Sandrasegaran K, Jennings SG, Aisen AM, Lin C, Sherman S, Rydberg MP. Diagnosis of chronic pancreatitis by using apparent diffusion coefficient measurements at 3.0-T MR following secretin stimulation. *Radiology* 2009; **252**: 418-425 [PMID: 19508986 DOI: 10.1148/radiol.2522081656]
38 **Taniguchi T**, Kobayashi H, Nishikawa K, Iida E, Michigami Y, Morimoto E, Yamashita R, Miyagi K, Okamoto M. Diffusion-weighted magnetic resonance imaging in autoimmune pancreatitis. *Jpn J Radiol* 2009; **27**: 138-142 [PMID: 19412681 DOI: 10.1007/s11604-008-0311-2]
39 **Taouli B**, Thakur RK, Mannelli L, Babb JS, Kim S, Hecht EM, Lee VS, Israel GM. Renal lesions: characterization with diffusion-weighted imaging versus contrast-enhanced MR imaging. *Radiology* 2009; **251**: 398-407 [PMID: 19276322 DOI: 10.1148/radiol.2512080880]
40 **Zhang J**, Tehrani YM, Wang L, Ishill NM, Schwartz LH, Hricak H. Renal masses: characterization with diffusion-weighted MR imaging--a preliminary experience. *Radiology* 2008; **247**: 458-464 [PMID: 18430878 DOI: 10.1148/radiol.2472070823]
41 **Paudyal B**, Paudyal P, Tsushima Y, Oriuchi N, Amanuma M, Miyazaki M, Taketomi-Takahashi A, Nakazato Y, Endo K. The role of the ADC value in the characterisation of renal carcinoma by diffusion-weighted MRI. *Br J Radiol* 2010; **83**: 336-343 [PMID: 19620174 DOI: 10.1259/bjr/74949757]
42 **Namimoto T**, Yamashita Y, Mitsuzaki K, Nakayama Y, Tang Y, Takahashi M. Measurement of the apparent diffusion coefficient in diffuse renal disease by diffusion-weighted echo-planar MR imaging. *J Magn Reson Imaging* 1999; **9**: 832-837 [PMID: 10373031]
43 **Thoeny HC**, De Keyzer F, Oyen RH, Peeters RR. Diffusion-weighted MR imaging of kidneys in healthy volunteers and patients with parenchymal diseases: initial experience. *Radiology* 2005; **235**: 911-917 [PMID: 15845792 DOI: 10.1148/radiol.2353040554]
44 **Yildirim E**, Kirbas I, Teksam M, Karadeli E, Gullu H, Ozer I. Diffusion-weighted MR imaging of kidneys in renal artery stenosis. *Eur J Radiol* 2008; **65**: 148-153 [PMID: 17537606 DOI: 10.1016/j.ejrad.2007.03.007]
45 **Chan JH**, Tsui EY, Luk SH, Fung SL, Cheung YK, Chan MS, Yuen MK, Mak SF, Wong KP. MR diffusion-weighted imaging of kidney: differentiation between hydronephrosis and pyonephrosis. *Clin Imaging* 2001; **25**: 110-113 [PMID: 11483420]
46 **Toyoshima S**, Noguchi K, Seto H, Shimizu M, Watanabe N. Functional evaluation of hydronephrosis by diffusion-weighted MR imaging. Relationship between apparent diffusion coefficient and split glomerular filtration rate. *Acta Radiol* 2000; **41**: 642-646 [PMID: 11092490]
47 **Tsushima Y**, Takahashi-Taketomi A, Endo K. Diagnostic utility of diffusion-weighted MR imaging and apparent diffusion coefficient value for the diagnosis of adrenal tumors. *J Magn Reson Imaging* 2009; **29**: 112-117 [PMID: 19097108 DOI: 10.1002/jmri.21616]
48 **Miller FH**, Wang Y, McCarthy RJ, Yaghmai V, Merrick L, Larson A, Berggruen S, Casalino DD, Nikolaidis P. Utility of diffusion-weighted MRI in characterization of adrenal lesions. *AJR Am J Roentgenol* 2010; **194**: W179-W185 [PMID: 20093571 DOI: 10.2214/AJR.09.2891]
49 **Ertan G**, Tekes A, Mitchell S, Keefer J, Huisman TA. Pediatric littoral cell angioma of the spleen: multimodality imaging including diffusion-weighted imaging. *Pediatr Radiol* 2009; **39**: 1105-1109 [PMID: 19597808 DOI: 10.1007/s00247-009-1339-x]
50 **Nakahashi M**, Sato N, Tsushima Y, Amanuma M, Endo K. Diffusion-weighted magnetic resonance imaging of the body in venous thrombosis: a report of four cases. *Abdom Imaging* 2008; **33**: 353-356 [PMID: 17624568 DOI: 10.1007/s00261-007-9252-y]
51 **Takahara T**, Imai Y, Yamashita T, Yasuda S, Nasu S, Van Cauteren M. Diffusion weighted whole body imaging with background body signal suppression (DWIBS): technical improvement using free breathing, STIR and high resolution 3D display. *Radiat Med* 2004; **22**: 275-282 [PMID: 15468951]
52 **Wang JW**, Zhao S, Liu Y, Li J, Xu LM. [Preliminary study on the validity of whole body diffusion-weighted imaging for the detection of malignant lesions]. *Zhonghua Zhongliu Zazhi* 2010; **32**: 304-308 [PMID: 20510086]
53 **Naganawa S**, Kawai H, Fukatsu H, Sakurai Y, Aoki I, Miura S, Mimura T, Kanazawa H, Ishigaki T. Diffusion-weighted imaging of the liver: technical challenges and prospects for the future. *Magn Reson Med Sci* 2005; **4**: 175-186 [PMID: 16543702]
54 **Koh DM**, Takahara T, Imai Y, Collins DJ. Practical aspects of assessing tumors using clinical diffusion-weighted imaging in the body. *Magn Reson Med Sci* 2007; **6**: 211-224 [PMID: 18239358]
55 **Le Bihan D**, Poupon C, Amadon A, Lethimonnier F. Artifacts and pitfalls in diffusion MRI. *J Magn Reson Imaging* 2006; **24**: 478-488 [PMID: 16897692 DOI: 10.1002/jmri.20683]

P- Reviewer Abou El-Ghar ME **S- Editor** Cheng JX
L- Editor Roemmele A **E- Editor** Zheng XM